Generation of Efficient Terahertz Radiation by Relativistic Self-Focusing of A Cosh-Gaussian Laser Beam in A Magnetized Plasma

Gunjan Purohit (gunjan75@gmail.com)
DAV Post Graduate College Dehradun https://orcid.org/0000-0002-2694-2659
Bineet Gaur
DAV Post Graduate College Dehradun
Pradeep Kothiyal
DAV Post Graduate College Dehradun
Amita Raizada
DAV Post Graduate College Dehradun

Research Article

Keywords: Cosh-Gaussian laser beam, magnetized plasma, relativistic nonlinearity, self-focusing, Terahertz (THz) radiation

Posted Date: December 29th, 2021

DOI: https://doi.org/10.21203/rs.3.rs-1195824/v1

Abstract

This paper presents a scheme for the generation of terahertz (THz) radiation by self-focusing of a cosh-Gaussian laser beam in the magnetized and rippled density plasma, when relativistic nonlinearity is operative. The strong coupling between self-focused laser beam and pre-existing density ripple produces nonlinear current that originates THz radiation. THz radiation is produced by the interaction of the cosh-Gaussian laser beam with electron plasma wave under the appropriate phase matching conditions. Expressions for the beamwidth parameter of cosh-Gaussian laser beam and the electric vector of the THz radiation have been obtained using higher-order paraxial theory and solved numerically. The self-focusing of the cosh-Gaussian laser beam and its effect on the generated THz amplitude have been studied for specific laser and plasma parameters. Numerical study has been performed on various values of the decentered parameter, incident laser intensity, magnetic field, and relative density. The results have also been compared with the paraxial region as well as the Gaussian profile of laser beam. Numerical results suggest that the self-focusing of the cosh-Gaussian laser beam and the amplitude of THz radiation increase in the extended paraxial region compared to the paraxial region. It is also observed that the focusing of the cosh-Gaussian laser beam in the magnetized plasma and the amplitude of the THz radiation increases at higher values of the decentered parameter.

1 Introduction

Terahertz (THz) radiation generation has been the most interesting topic of research in recent years. THz radiation sources have wide applications in the fields of THz time-domain spectroscopy, material characterization, explosives science, imaging, topography, medical diagnostics, security identification, etc. (Ferguson and Zhang 2002; Shen et al. 2005; Pickwell and Wallace 2006; Mittleman et al. 1996). Various schemes such as photoconductive antennas, optical rectification, quantum cascade lasers, and the semiconductors and electro-optic crystals (e.g., ZnSe, ZnTe, GaSe and $LiNbO_3$) have been used to generate THz radiation (Tani et al. 2002; Chen et al. 2011; Vodopyanov 2008; Lee et al. 2000). But due to some limitations of these schemes such as low conversion efficiency, narrow bandwidth of emitted THz radiation, and material breakdown in intense laser pulses, high energy THz radiation is not sufficiently generated. These limitations can be overcome by the use of plasma. Plasma is an attractive medium for THz radiation production because it is able to handle very high laser powers without any constraint of medium breakdown.

The production of THz radiation by laser plasma interaction has been the subject of intense study for the past two decades (Liao and Li 2019; Tonouchi 2007). Several schemes have been proposed to produce efficient THz radiation through laser–plasma interactions. Coherent Thz radiation has been measured by laser accelerated electron bunches moving from plasma to vacuum (Leemans et al. 2003; Leemans et al. 2004; Tilborg et al. 2006). Coherent radiation in the range of 0.3–3 THz generated from femtosecond electron bunches at the plasma-vacuum boundary via transition radiation has been experimentally observed (Leemans et al. 2003). Terahertz radiation can also be generated from radiation generated by a two-color laser pulse (fundamental and second harmonic field) during gas ionization (Kim et al. 2007; Kim et al. 2008; Kim 2009). It has been reported that THz energy of more than 5 μJ is generated through this mechanism (Kim et al. 2008). THz radiation has also been generated by laser pulses propagating in short corrugated plasma channels (Antonsen et al. 2007; Pearson et al. 2011; Miao et al. 2017). It is found that a pulse energy of 0.5 J generates a terahertz energy of 6 mJ through the corrugated plasma channel (Pearson et al. 2011). These types of channels can also be used to generate THz radiation by bunched electron beams. In addition, high power THz radiation has been generated from short laser pulses in the plasma through various mechanisms (Chen 2013; Sharma and Singh 2014; Malik et al. 2020; Koulouklidis et al. 2020).

In recent years THz radiation by self-focusing/filamentation of an intense laser beam in plasma has been studied. The main motive is to increase the conversion efficiency of THz radiation. Self-focusing of an intense laser pulse into the plasma increases the efficiency of THz radiation. Hamster et al. (1994) shown experimentally that plasmas produced by high intensity lasers generates coherent Thz radiation. Mun et al. (2007) observed an intense Thz radiation from a relativistic plasma on metal and plastic targets irradiated with 10-TW, 30-fs laser pulses. Hussain et al. (2014; 2016) proposed a scheme for the generation of Thz radiation by ponderomotive/relativistic self-focusing of a hollow Gaussian laser beam in a collissionless magnetized rippled density plasma. They found that these schemes increase the power level of the THz wave to the order of Gigawatts. Kumar et al. (2015) studied the effect of self-focusing of an amplitude- modulated Gaussian laser beam on THz generation in rippled density plasma. They observed that when the self-focusing effect is taken into account, the amplitude of the generated THz wave increases significantly. Miao et al. (2016) developed a mechanism for ponderomotive driven resonant THz transition radiation generated at plasma boundaries and found that broad-band THz radiation is generated with frequencies up to the maximum plasma frequency. Liao et al. (2016) reported intense THz radiation from relativistic laser–plasma interactions under various experimental conditions. Their results indicate that relativistic laser plasma is a promising source of intense THz radiation. Rawat et al. (2017) studied the self-focusing effect of hollow Gaussian laser beam on the generation of THz radiation in a collisionless magnetized plasma, where relativistic and ponderomotive nonlinearities are operate together. Amouamouha et al. (2020) proposed a scheme to generate THz radiation at the modulation frequency, which is based on the pondermotive self- focusing of an amplitude modulated super Gaussian laser beam in preformed ripple density plasma. This study has been performed in the higher-order paraxial region, where pondermotive nonlinearity is operative. They found that the efficiency of THz radiation reaches 6.5%. Recently, Gupta and Jain (2021) have investigated Thz radiation production by a super-Gaussian laser pulse in a magnetized plasma. They observed that stable THz radiation is generated with a maximum field strength of 1 GV/cm and a relatively broad spectrum spanning 50 THz, which corresponds to a conversion efficiency for a magnetic field strength of 1 T. Other recent studies of Thz radiation production in laser produced plasma have been reported in the literature (Tripathi et al. 2010; Singh et al. 2012; Kumar et al. 2016).

Various profiles of laser beams such as Gaussian, super Gaussian, hollow-Gaussian and triangular profiles etc. have been used to generate THz radiation in plasma in these studies. Such beams have different types of irradiances across their wavefront, which exhibit different characteristics in plasma. Recently, flat-top decentred cosh-Gaussian laser beams have attracted much attention due to their higher efficient power and attractive applications (Konar et al. 2007; Nanda and Kant 2014; Rawat and Purohit 2019). The most important specialty of the cosh-Gaussian laser beam is that it becomes focused before the Gaussian laser beam in the plasma. Furthermore, most studies of THz radiation schemes based on laser–plasma interactions have used the paraxial-ray approximation (Akhmanov et al. 1968). But at high intensities the paraxial-ray theory is not sufficiently accurate because this theory does not describe the variation of the radial profile of the beam from the initial to the ring position. The extended-paraxial ray approximation (Bonnaud et al. 1994; Sodha and Faisal 2008) more accurately describes the propagation of an intense laser beam in plasma than the paraxial ray approximation. At higher laser intensities, the relativistic nonlinearity functional occurs in the plasma. Therefore, it would be interesting to investigate the self-focusing effect of cosh-Gaussian laser beam in plasma with relativistic nonlinearity on the generation of THz radiation under the extended- paraxial approximation theory.

This paper presents a model for the production of THz radiation by relativistic self-focusing of an intense cosh-Gaussian laser beam in a magnetized plasma. This study is carried out under the extended-paraxial ray approximation, which is based on the expansion of the eikonal and nonlinear dielectric constant up to the fourth power of r, where r is the distance from the axis of the beam. Due to the nonlinear coupling between the cosh-

Gaussian laser beam and the electron plasma wave (EPW) in a rippled density plasma, THz radiation is emitted. The ripple in plasma density plays a major role for the production of THz radiation as it provides the necessary conditions for phase matching. The paper is structured as follows: In section 2, the self-focusing equation of an intense cosh-Gaussian laser beam through a magnetized plasma in the presence of relativistic nonlinearity is obtained using a higher-order paraxial ray approximation. In the same section, the expression for the nonlinear effective dielectric constant of plasma in the presence of relativistic nonlinearity is obtained. Section 3 presents the analysis for the nonlinear current density and the emitted THz radiation amplitude. Section 4 presents a discussion of numerical results for the relevant parameters. Finally, Section 5 contains conclusions.

2 Relativistic Self-focusing Of Cosh-gaussian Laser Beam In Magnetized Plasma

Consider the propagation of a cosh Gaussian laser beam (CGB) of angular frequency (ω_{0+}) and wave vector (k_{0+}) along the direction of the static magnetic field in a collisionless magneto plasma. The external applied static magnetic field (B_0) is perpendicular to the propagation direction (towards z-axis) of laser beam. The electric field of cosh-Gaussian laser beam can be written as

$$E_{0+} = E_x + iE_y = A_{0+}(r, z)\exp\left[i\left(\omega_{0+}t - k_{0+}z\right)\right]$$

1

where+ sign denotes the right circular mode of propagation, A_{0+} is the amplitude of the electric field, and k_{0+} is the propagation wave vector of the laser beam.

The initial amplitude of the cosh-Gaussian laser beam at $z = 0$ is given by (Lü et al. 1999; Konar et al. 2007)

$$\left(A_{0+}\right) = \frac{E_{00+}}{2}e^{\frac{b^2}{4}}\left\{\exp\left[-\left(\frac{r}{r_0}+\frac{b}{2}\right)^2\right] + \exp\left[-\left(\frac{r}{r_0}-\frac{b}{2}\right)^2\right]\right\}$$

2

where E_{00+} is the amplitude of cosh-Gaussian laser beam for the central position at $r = z = 0$, b is the decentred parameter of the beam, r is the radial coordinate of the cylindrical coordinate system, and r_0 is the initial beam width.

The dielectric constant (ϵ_+) corresponding to wave propagation vector (k_{0+}) is given by

$$\epsilon_+(r, z) = 1 - \frac{\omega_{pe}^2}{\omega_{0+}^2}\left(1 - \frac{\omega_{ce}}{\omega_{0+}}\right)^{-1}$$

3

where $\omega_{pe} = \left(\frac{4\pi n_0 e^2}{m_e}\right)^{1/2}$ is the electron plasma frequency, and $\omega_{ce} = \frac{eB_0}{m_e c}$ is the electron cyclotron frequency respectively, e is the electronic charge, m_e is the rest mass of electron, c is the light velocity and n_0 is the electron

density of the plasma in the absence of laser beam.

The relativistic motion equation of an electron in the presence of a static magnetic field B_0 and intense laser field E_{0+} is written as (Hassoon et al. 2010)

$$m_e \frac{\partial}{\partial t} \gamma v_{0+} = -e\left(E_{0+} + \frac{1}{c}(v_{0+} \times B_0)\right)$$

4

where γ is the relativistic factor and v_{0+} is the oscillation velocity imparted by laser beam. The Lorentz force factor $\left(-\frac{1}{c}(v_{0+} \times B_0)\right)$ is not considered here because for ultra-short intense laser pulses relativistic nonlinearity becomes set up almost instantaneously.

The oscillatory drift velocity of electrons $\left(v_{0+}\right)$ for right circularly polarized mode of relativistic laser beam is given by

$$v_{0+} = v_x + iv_y = \frac{ieE_{0+}}{m_e \gamma \omega_{0+}\left(1 - \frac{\omega_{ce}}{\gamma \omega_{0+}}\right)}$$

5

The relativistic factor (γ) is given by

$$\gamma \approx 1 + \alpha_+ A_{0+} A_{0+}^*$$

6

where $\alpha_+ = \frac{e^2}{2m_e^2 \omega_{0+}^2 c^2}\left(1 - \frac{\omega_{ce}}{\omega_{0+}}\right)^{-2}$

The propagation of cosh-Gaussian laser beam in magnetized plasma is governed by the general wave equation (Sodha et al. 1974)

$$\frac{\partial^2 E_{0+}}{\partial z^2} - \nabla(\nabla . E_{0+}) + \frac{\omega_{0+}^2}{c^2} \epsilon_+(r, z) E_{0+} = 0$$

7

where ε_+ is the effective dielectric constant of the plasma.

The effective dielectric constant (ε_+) of the plasma in the presence of relativistic nonlinearity for the right circularly polarized laser beam is given by

$$\epsilon_+ = \epsilon_{xx} - i\epsilon_{xy} = 1 - \frac{\omega_{pe}^2}{\omega_{0+}^2 \gamma}\left(1 - \frac{\omega_{ce}}{\omega_{0+}\gamma}\right)^{-1}$$

8

where ε_{xx} and ε_{xy} are the components of plasma dielectric constant tensor. Putting the value of relativistic factor (γ) in above equation, one may get

$$\epsilon_+ = 1 - \frac{\omega_{pe}^2}{\omega_{0+}^2}\left(1 - \frac{\omega_{ce}}{\omega_{0+}}\right)^{-1} + \frac{\omega_{pe}^2}{\omega_{0+}^2}\left(1 - \frac{\omega_{ce}}{\omega_{0+}}\right)^{-2}\alpha_+ A_{0+}A_{0+}^*$$

9

By using Eq. (1), Eq. (7) can be written in terms of A_{0+} is as

$$\frac{\partial^2 A_{0+}}{\partial z^2} - 2ik_{0+}\frac{\partial A_{0+}}{\partial z} - iA_{0+}\frac{\partial k_{0+}}{\partial z}\frac{1}{2}\left(1 + \frac{\epsilon_{0+}}{\epsilon_{0zz}}\right) + \frac{\omega_{0+}^2}{c^2}\left[\epsilon_+\left(r, z\right) - \epsilon_{0+}\right]A_{0+} = 0$$

10

where

$$\epsilon_{0+} = 1 - \frac{\omega_{pe}^2}{\omega_{0+}^2}$$

The solution of Eq. (10) can be written as

$$A_{0+} = A_{00+}(r, z)exp\left[-ik_{0+}S_+(r, z)\right]$$

11

where A_{00+} is a real function, $k_{0+} = \frac{\omega_{0+}}{c}\left(\epsilon_{0+}\right)^{1/2}$, and S_+ is the eikonal which shows slight converging/diverging behavior of the beam in the plasma.

The expansion of $\epsilon_+(r, z)$ under the extended-paraxial region can be written as

$$\epsilon_+(r, z) = \epsilon_{0+}(z) - \frac{r^2}{r_0^2}\epsilon_{2+}(z) - \frac{r^4}{r_0^4}\epsilon_{4+}(z)$$

12

where ϵ_{0+}, ϵ_{2+}, and ϵ_{4+} are the expansion coefficients. Substituting Eqs. (11) and (12) in Eq. (10) and neglecting the term $\frac{\partial^2 A_{0+}}{\partial z^2}$, real and imaginary parts can be obtained as

$$2\left(\frac{\partial S_+}{\partial z}\right)+\frac{2S_+}{k_{0+}}+\left(\frac{\partial S_+}{\partial r}\right)^2=\frac{1}{k_{0+}^2A_{00+}}\left(1+\frac{\epsilon_{0+}}{\epsilon_{0zz}}\right)\left(\frac{\partial^2A_{00+}}{\partial r^2}+\frac{1}{r}\frac{\partial A_{00+}}{\partial r}\right)-\frac{r^2\epsilon_{2+}(z)}{r_0^2\epsilon_{0+}(z)}-\frac{r^4\epsilon_{4+}(z)}{r_0^4\epsilon_{0+}(z)}$$

13

and

$$\frac{\partial A_{00+}^2}{\partial z}+A_{00+}^2\left(1+\frac{\epsilon_{0+}}{\epsilon_{0zz}}\right)\left(\frac{\partial^2S_+}{\partial r^2}+\frac{1}{r}\frac{\partial S_+}{\partial r}\right)+\frac{\partial A_{00+}^2}{\partial r}\frac{\partial S_+}{\partial r}+\frac{A_{00+}^2}{k_{0+}}\frac{dk_{0+}}{dz}=0$$

14

The solution of Eqs. (13) and (14) for cosh-Gaussian beam under extended-paraxial theory can be written as (Sodha and Faisal 2008: Purohit et al. 2021)

$$A_{00+}^2(r,z)=\frac{E_{00+}^2}{4f_{0+}^2}exp\left(\frac{b^2}{2}\right)\times\left(\exp\left[-\left(\frac{r}{r_of_{0+}}+\frac{b^2}{2}\right)^2\right]+\exp\left[-\left(\frac{r}{r_of_{0+}}-\frac{b^2}{2}\right)^2\right]\right)^2$$

$$\times\left(1+\frac{r^2}{r_0^2f_{0+}^2}a_2(z)+\frac{r^4}{r_0^4f_{0+}^4}a_4(z)\right)$$

15

and

$$S_+(r,z)=S_{0+}(z)+\frac{r^2}{r_0^2}S_{2+}(z)+\frac{r^4}{r_0^4}S_{4+}(z)$$

16

where $a_2(z)$and $a_4(z)$are the coefficients of $r^2$and r^4, which characterizing the extended-paraxial region contribution to the beam intensity and indicating the departure of the beam from the Gaussian nature, $S_{0+}(z)$is the axial phase shift, $S_{2+}(z)$ and $S_{4+}(z)$ indicate the spherical curvature of the wavefront and the wavefront departure from the spherical nature respectively.

Substituting the value of $A_{00+}^2$and $S_+$from Eqs. (15) and (16) in Eq. (14), and equating the coefficients of r^0, r^2, and r^4 on both sides of the resulting equation, one can obtain

$$S_2(z)=\frac{r^2}{f_{0+}^2}\left(1+\frac{\epsilon_{0+}}{\epsilon_{0zz}}\right)^{-1}\frac{df_{0+}}{dz}$$

17

$$\frac{da_2}{d\xi} = -16S_{04+}f_{0+}^2\left(1+\frac{\epsilon_{0+}}{\epsilon_{0zz}}\right)$$

18

and

$$\frac{da_4}{d\xi} = 8S_{04+}f_{0+}^2\left(b^2+3a_2-2\right)\left(1+\frac{\epsilon_{0+}}{\epsilon_{0zz}}\right)$$

19

where

$$S_{04+} = S_{4+}\left(\frac{\omega_{0+}}{c}\right)$$

20

The relation between a_4 and a_2 can be obtained by eliminating S_{04+} in Eqs. (18) and (19) and integrating the result with the initial conditions $a_4 = 0$ and $a_2 = 0$ at $\xi = 0$ i.e.

$$a_4 = \frac{\left(4b^2a_2+3a_2^2-4a_2\right)}{4}$$

21

After replacing Eq. (21) in Eq. (15), one may obtain the amplitude of cosh-Gaussian laser beam as:

$$A_{00+}^2(r,z) = \frac{E_{00+}^2}{4f_{0+}^2}exp\left(\frac{b^2}{2}\right)\times\left(\exp\left[-\left(\frac{r}{r_of_{0+}}+\frac{b^2}{2}\right)^2\right]+\exp\left[-\left(\frac{r}{r_of_{0+}}-\frac{b^2}{2}\right)^2\right]\right)^2$$

$$\times\left(1+\frac{r^2}{r_0^2f_{0+}^2}a_2(z)+\frac{r^4}{r_0^4f_{0+}^4}\frac{\left(4b^2a_2+3a_2^2-4a_2\right)}{4}\right)$$

22

Similarly, by replacing Eqs. (15) and (16) in Eq. (13) and equating the coefficients of r^2 and r^4 in the resulting equation, following equations have been obtained for the beam width parameter (f_{0+}) of cosh-Gaussuan laser beam and for S_{04+}:

$$\frac{d^2 f_{0+}}{d\xi^2} = \left(1 + \frac{\epsilon_{0+}}{\epsilon_{0zz}}\right)^2 \frac{\chi_2}{\epsilon_{0+} f_{0+}^3} - \left(1 + \frac{\epsilon_{0+}}{\epsilon_{0zz}}\right) \frac{2\epsilon_{2+} f_{0+} \rho^2}{\epsilon_{0+}} (23)$$

and

$$\frac{dS_{04+}}{d\xi} = \frac{1}{4}\left(1 + \frac{\epsilon_{0+}}{\epsilon_{0zz}}\right) \frac{\chi_4}{\epsilon_{0+} f_{0+}^6} - \frac{\epsilon_{4+}\rho^2}{2\epsilon_{0+}} - \frac{2S_{04+}}{f_{0+}} \frac{df_{0+}}{d\xi} (24)$$

where

$$\chi_2 = 8a_4 + 2a_2 b^2 - 3a_2^2 - 4a_2 - \frac{b^4}{3} - 4b^2 + 4$$

and

$$\chi_4 = 4a_2^3 + 4a_2^2 + 4a_4 b^2 - 2a_2^2 b^2 - 8a_4 - 14a_2 a_4 - 2a_2 \frac{b^4}{3} + 17\frac{b^4}{6} + \frac{b^6}{12}$$

$\xi = \frac{cz}{r_0^2 \omega_{0+}}$ is the dimensionless distance of propagation, and $\rho = \frac{r_0 \omega_{0+}}{c}$ is dimensionless initial beam width of the beam. The first term on the right-hand side in Eq. (23) represents the diffraction effect, and the second term is a nonlinear term on the account of the relativistic nonlinearity, including the magnetic field.

2.1 Evaluation of the Effective Dielectric Constant

In order to solve the value of the effective dielectric constant in extended-paraxial region, one can expand the solution for A_{00+}^2 asapolynomialin r^2 and r^4 as

$$A_{00+}^2 = g_0 + g_2 r^2 + g_4 r^4$$

25

where

$$g_0 = \frac{E_{00+}^2}{f_{0+}^2}$$

$$g_2 = g_0 \frac{\left(b^2 + a_2 - 2\right)}{r_0^2 f_{0+}^2}$$

and

$$g_4 = g_0 \frac{\left(a_4 + a_2 b^2 - 2a_2 + \frac{b^4}{3} - 2b^2 + 2\right)}{r_0^4 f_{0+}^4}$$

To write ε_+ explicitly in the extended-paraxial approximation, γ can be expanded as

$$\gamma = \gamma_0 + \gamma_2 \frac{r^2}{r_0^2} + \gamma_4 \frac{r^4}{r_0^4}$$

26

where the values of {\gamma }_{0}, {\gamma }_{2 }and {\gamma }_{4} can be obtained from Eq. (6) are as:

{\gamma }_{0}={\left(1+\frac{{\gamma }_{0}^{2}\alpha {g}_{0}}{{\left({\gamma }_{0}- \frac{{\omega }_{ce}}{{\omega }_{0+}}\right)}^{2}}\right)}^{1/2}
{\gamma }_{2}=\frac{\alpha {g}_{2}}{2\left({\gamma }_{0}- \frac{{2\omega }_{ce}}{{\omega }_{0+}} - \frac{2{\omega }_{ce}}{{\omega }_{0+}{\gamma }_{0}^{2}} + \frac{2{\omega }_{ce}^{2}}{{\omega }_{0+}^{2}{\gamma }_{0}^{3}}\right)}

and

{\gamma }_{4}=\frac{\alpha {g}_{4}+\left(3 - \frac{{\omega }_{ce}}{{\omega }_{0+{\gamma }_{0}}} -\frac{{2\omega }_{ce}^{2}}{{\omega }_{0+}^{2}{\gamma }_{0}^{2}} + \frac{{\omega }_{ce}^{2}}{{\omega }_{0+}^{2}{\gamma }_{0}^{4}}\right)}{2\left({\gamma }_{0}- \frac{{\omega }_{ce}}{{\omega }_{0+}} - \frac{{\omega }_{ce}}{{\omega }_{0+}{\gamma }_{0}^{2}} + \frac{{\omega }_{ce}^{2}}{{\omega }_{0+}^{2}{\gamma }_{0}^{3}}\right)}

By substituting the value of γ from Eq. (26) in Eq. (8), expanding ε_+ as a series of power \frac{r}{{r}_{0}}, and comparing the result with Eq. (13), one obtains

{\epsilon }_{0+}\left(z\right)=1-\frac{{\omega }_{pe}^{2}}{{\omega }_{0+}^{2}}\frac{1}{\left({\gamma }_{0 }- \frac{{\omega }_{ce}}{ {\omega }_{0+}}\right)}
27
{\epsilon }_{2+}\left(z\right)=\frac{{\omega }_{pe}^{2}}{{\omega }_{0+}^{2}}\frac{{\gamma }_{2 }}{{\left({\gamma }_{0 }-\frac{{\omega }_{ce}}{ {\omega }_{0+}}\right)}^{2}}
28

and

{\epsilon }_{4+}\left(z\right)=\frac{2{\omega }_{pe}^{2}}{{\omega }_{0+}^{2}}\left[\frac{\left({\gamma }_{0 }- \frac{{\omega }_{ce}}{ {\omega }_{0+}}\right){\gamma }_{4}-{\gamma }_{2}^{2}}{{\left({\gamma }_{0 }-\frac{{\omega }_{ce}}{ {\omega }_{0+}}\right)}^{3}}\right]
29

3 Generation Of Terahertz Radiation

The self-focused cosh-Gaussian laser beam excites terahertz radiation in magnetized plasma. Now we consider propagation of a cosh-Gaussian laser beam (whose electric field is given by Eq. (1)) through rippled density plasma

(which is presumed to exist across the magnetic field). Due to strong nonlinear coupling between cosh-Gaussian laser beam (E_{0+}, ω_{0+},\overrightarrow{k}$_{0+}$) and electron plasma wave (\overrightarrow{E}$_p$, ω_p, \overrightarrow{k}$_p$), terahertz radiation (\overrightarrow{E}$_{t+}$, ω_t, \overrightarrow{k}$_t$) is generated at the difference frequency of cosh-Gaussian laser beam and electron plasma wave. The ripple density plasma fulfils the requirement of momentum phase matching that paves the way for efficient terahertz radiation generation. The required phase matching conditions for the emission of THz radiation are: {\omega }_{0+}={\omega }_{p}+{\omega }_{t+} and {k}_{0+}={k}_{p}+{k}_{t}, where \overrightarrow{E}$_p$, ω_p, k_p and \overrightarrow{E}$_{t+}$, ω_{t+}, k_t are the electric fields, frequencies and wave vectors of electron plasma wave and terahertz wave, respectively.

The electric field of an electron plasma wave and terahertz wave can be represented as (Hassan et al. 2012)

\overrightarrow{E} $_p$=\widehat{z}{E}_{p}expi({\omega }_{p}t-{k}_{p}z) (30)

and

\overrightarrow{E} $_{t+}$=\widehat{r}{E}_{t0+}expi({\omega }_{t+}t-{k}_{t+}z) (31)

where {E}_{t0+} is amplitude of the right circular polarized THz field, and \widehat{r}=\widehat{x}+i\widehat{y} (\widehat{x} and \widehat{y} are the unit vectors along the *x*- and *y*-axis respectively).

When an intense cosh-Gaussian laser beam is propagating in the ripple density magnetoplasma, the total number density of electrons can be expressed as

n={n}_{0}+{\tilde{n}}_{p}\text{e}\text{x}\text{p}\left[{i(\omega }_{p}t-{k}_{p}z)\right]+{n}_{q}\text{e}\text{x}\text{p}(-iqz) 32

where {n}_{0}, {\tilde{n}}_{p}, and {n}_{q} are background density, density perturbation due to electron plasma wave, and density of ripple, respectively.

The wave equation for THz generation in magnetized plasma can be written as (Shukla and Sharma 1982)

{\nabla }^{2}\overrightarrow{E} $_{t+}$ =\frac{1}{{c}^{2}}\frac{{\partial }^{2}}{{\partial t}^{2}}\overrightarrow{E} $_{t+}$ + \frac{4\pi }{{c}^{2}}\frac{\partial }{\partial t}\overrightarrow{J} $_{t+}$ (33)

where \overrightarrow{J}$_{t+}$ (=\overrightarrow{J}$_{L+}$ +\overrightarrow{J}$_{NL+}$) is the total current density vector in the presence of low frequency electric field \overrightarrow{E}$_{t+}$.

The current density can be evaluated by the following equations:

1. Continuity equation:

\frac{\partial {n}_{j}}{\partial t}+\nabla \bullet ({n}_{j}\overrightarrow{\upsilon } $_j$)=0 (34)

1. Momentum transfer equation:

{m}_{j}\left(\gamma \frac{\partial }{\partial t}{\overrightarrow{\upsilon }}_{j}+({\overrightarrow{\upsilon }}_{j}\bullet \nabla){\overrightarrow{\upsilon }}_{j}\right)=-\text{e}\left({\overrightarrow{E}}_{t+}+\frac{1}{c}{\overrightarrow{\upsilon }}_{j}\times (\overrightarrow{B}+{\overrightarrow{B}}_{0}) \right) 35

where n_j, m_j, and {\overrightarrow{\upsilon }}_{j}are the number density, mass and the fluid velocity of electrons and ions ($j = e, i$) respectively, \overrightarrow{B} is the magnetic field of terahertz wave, and {\overrightarrow{B}}_{0} is static background magnetic field.

Due to the electric field of electron plasma wave ($\overrightarrow{E}_p$), the electrons acquire relativistic oscillating velocity {\overrightarrow{\upsilon }}_{p} i.e.

{\overrightarrow{\upsilon }}_{p}=-\frac{ie{\overrightarrow{E}}_{1}}{{m}_{e}\gamma {\omega }_{p}}
.

Using continuity equation, we obtain the following expression

{\overrightarrow{\upsilon }}_{p}=\frac{{\omega }_{p}}{{\overrightarrow{k}}_{p}}\mu
36

which gives the relation between the density perturbation and the electron velocity, where \mu =\frac{{\tilde{n}}_{p}}{{n}_{0}} is the ratio between perturbed density {\tilde{n}}_{p}and background plasma density n_0 i. e. normalized density of the electron plasma wave.

The linear current density ($\overrightarrow{J}_{L+}$) and the nonlinear current density ($\overrightarrow{J}_{NL+}$) could be expressed by the following expressions:

{\overrightarrow{J}}_{L+}=-e{n}_{0}{\overrightarrow{\upsilon }}_{L+}^{e}+e{n}_{0}{\overrightarrow{\upsilon }}_{L+}^{i}
37

and

{\overrightarrow{J}}_{NL+}=-e{\tilde{n}}_{p}^{*}{\overrightarrow{\upsilon }}_{0+}-e{n}_{0}{\overrightarrow{\upsilon }}_{NL+}^{e}=-e{n}_{q}{\overrightarrow{\upsilon }}_{NL+}^{e}
38

where {\overrightarrow{\upsilon }}_{L+}^{e} and {\overrightarrow{\upsilon }}_{L+}^{i} are linear components of electron and ion velocities, {\overrightarrow{\upsilon }}_{0+} is the electron-oscillating velocity of laser beam, and {\overrightarrow{\upsilon }}_{NL+}^{e} is the nonlinear component of the electron velocity.

The electron and the ion linear velocities are obtained by solving the momentum equation (Eq. 35) with respect to terahertz wave. The linear velocity for ion is as

{\overrightarrow{\upsilon }}_{L+}^{e}=\frac{i{eE}_{t+}}{{m}_{e}\gamma {\omega }_{t+}}{\left(1-\frac{{\omega }_{ce}}{{\omega }_{t+}\gamma }\right)}^{-1}
39

and the linear velocity for electron is

{\overrightarrow{\upsilon }}_{L+}^{i}=\frac{i{eE}_{t+}}{{m}_{i}\gamma {\omega }_{t+}}{\left(1-\frac{{\omega }_{ci}}{{\omega }_{t+}\gamma }\right)}^{-1}
40

where ω_{ce} and ω_{ci} are electron –cyclotron frequency and ion–cyclotron frequency respectively.

The nonlinear component of the electron velocity ({\overrightarrow{\upsilon }}_{NL+}^{e}) is produced by the interaction between the laser beam and density ripple, as well as the magnetic field of the laser beam {\overrightarrow{B}}_{+}=\left(\frac{c{k}_{0+}}{{\omega }_{0}}\right)\widehat{z}\times {\overrightarrow{E}}_{0+}. Putting the value of {\overrightarrow{B}}_{+} in momentum equation, one obtains

{\overrightarrow{\upsilon }}_{NL+}^{e}=-\frac{ie{k}_{0+}{\overrightarrow{\upsilon }}_{p}^{*}{\overrightarrow{E}}_{0+}}{2{m}_{e}\gamma {\omega }_{0+}^{2}{\omega }_{t+}\left(1-\frac{{\omega }_{ce}}{{\omega }_{0+}\gamma }\right)\left(1-\frac{{\omega }_{ce}}{{\omega }_{t+}\gamma }\right)}\left(\frac{{\omega }_{ce}}{\gamma }\right)
41

where {\overrightarrow{\upsilon }}_{p}^{*} is the complex conjugate of the velocity {\overrightarrow{\upsilon }}_{p}.

Here, the ion contribution to nonlinearity is neglected because of its heavy mass. By replacing the velocity components of electron and ion from Eqs. (39) and (40) in Eq. (37), we obtain the expression of linear current density is as

{\overrightarrow{J}}_{L+}=-\frac{i{\omega }_{pe}^{2}{\overrightarrow{E}}_{t+}}{4\pi \gamma {\omega }_{t+}}{\left(1-\frac{{\omega }_{ce}}{{\omega }_{t+}\gamma }\right)}^{-1}{\left(1-\frac{{\omega }_{ci}}{{\omega }_{t+}\gamma }\right)}^{-1}
42

Nonlinear current density is produced by coupling of oscillatory velocity of laser beam and the nonlinear electron velocity. Substituting Eq. (41) in Eq, (38), we get

{\overrightarrow{J}}_{NL+}=-\frac{i{\omega }_{pe }^{2}{\omega }_{p}{k}_{0+}{\omega }_{ce}{\mu }^{*}}{8\pi {\gamma }^{2}{\omega }_{0+}^{2}{\omega }_{t+}{k}_{p}}{\overrightarrow{E}}_{0+}{\left(1-\frac{{\omega }_{ce}}{{\omega }_{t+}\gamma }\right)}^{-1}{\left(1-\frac{{\omega }_{ce}}{{\omega }_{0+}\gamma }\right)}^{-1}\left(\frac{{n}_{q}}{{n}_{0}}\right)
43

Using Eqs. (42) and (43) in Eq. (33), one gets the following equation for the terahertz field

\frac{{\partial }^{2}{\overrightarrow{E}}_{t+}}{{\partial z}^{2}}+\frac{{\omega }_{t+}^{2}}{{c}^{2}}\left[1-\frac{{\omega }_{p0}^{2}}{\gamma {\omega }_{t+}^{2}}{\left(1-\frac{{\omega }_{ce}}{{\omega }_{t+}\gamma }\right)}^{-1}{\left(1-\frac{{\omega }_{ci}}{{\omega }_{t+}\gamma }\right)}^{-1}\right]
{\overrightarrow{E}}_{t+}=\left(\widehat{x}+i\widehat{y}\right)
\times \frac{{\omega }_{pe }^{2}{\omega }_{p}{k}_{0+}{\omega }_{ce}{\mu }^{*}}{2{\omega }_{0+}^{2}{c}^{2}{\gamma }^{2}{k}_{p}}{\left(1-\frac{{\omega }_{ce}}{{\omega }_{t+}\gamma }\right)}^{-1}{\left(1-\frac{{\omega }_{ce}}{{\omega }_{0+}\gamma }\right)}^{-1}\left(\frac{{n}_{q}}{{n}_{0}}\right)\frac{{E}_{00+}}{2{f}_{0+}}\text{e}\text{x}\text{p}\left(\frac{{b}^{2}}{4}\right)\times {\left(1+\frac{{r}^{2}}{{r}_{0}^{2}{f}_{0+}^{2}}{a}_{2}\left(z\right)+\frac{{r}^{4}}{{r}_{0}^{4}{f}_{0+}^{4}}{a}_{4}\left(z\right)\right)}^{\frac{1}{2}}\times \left(\text{e}\text{x}\text{p}\left[-{\left(\frac{r}{{r}_{0}{f}_{0+}}+\frac{b}{2}\right)}^{2}\right]+\text{e}\text{x}\text{p}\left[-{\left(\frac{r}{{r}_{0}{f}_{0+}}+\frac{b}{2}\right)}^{2}\right]\right)
44

Further, the above equation can be simplified by calculating relativistic factor (γ). Eq. (44) can be rewritten as:

\frac{{\partial }^{2}{\overrightarrow{E}}_{t+}}{{\partial z}^{2}}+\frac{{\omega }_{t+}^{2}}{{c}^{2}}\left[1-\frac{{\omega }_{p0}^{2}}{{\omega }_{t+}^{2}}{\left(1-\frac{{\omega }_{ce}}{{\omega }_{t+}}\right)}^{-1}{\left(1-\frac{{\omega }_{ci}}{{\omega }_{t+}}\right)}^{-1}+{\alpha }_{t+}\right]
{\overrightarrow{E}}_{t+}=\left(\widehat{x}+i\widehat{y}\right)\left[\frac{{\omega }_{pe }^{2}{\omega }_{p}{k}_{0+}{\omega }_{ce}{\mu }^{*}}{2{\omega }_{0+}^{2}{c}^{2}{\gamma }^{2}{k}_{p}}{\left(1-\frac{{\omega }_{ce}}{{\omega }_{t+}}\right)}^{-1}{\left(1-\frac{{\omega }_{ce}}{{\omega }_{0+}}\right)}^{-1}\left(\frac{{n}_{q}}{{n}_{0}}\right)+{\alpha }_{tt+}\left(\frac{{n}_{q}}{{n}_{0}}\right)\right]\times \frac{{E}_{00+}}{2{f}_{0+}}\text{e}\text{x}\text{p}\left(\frac{{b}^{2}}{4}\right)\times {\left(1+\frac{{r}^{2}}{{r}_{0}^{2}{f}_{0+}^{2}}{a}_{2}\left(z\right)+\frac{{r}^{4}}{{r}_{0}^{4}{f}_{0+}^{4}}{a}_{4}\left(z\right)\right)}^{\frac{1}{2}}\times \left(\text{e}\text{x}\text{p}\left[-{\left(\frac{r}{{r}_{0}{f}_{0+}}+\frac{b}{2}\right)}^{2}\right]+\text{e}\text{x}\text{p}\left[-{\left(\frac{r}{{r}_{0}{f}_{0+}}+\frac{b}{2}\right)}^{2}\right]\right)
45

where {\alpha }_{t+}and {\alpha }_{tt+} represent the contribution of relativistic mass increase to the growth of THz radiation, and {f}_{0+} is the beam width parameter of cosh-Gaussian laser beam governed by the Eq. (23). The values of {\alpha }_{t+}and {\alpha }_{tt+} are given as

{\alpha }_{t+}=\frac{{\omega }_{p0}^{2}}{{c}^{2}}\frac{1}{{\left(1-\frac{{\omega }_{ce}}{{\omega }_{t+}}\right)}^{2}{\left(1+\frac{{\omega }_{ci}}{{\omega }_{t+}}\right)}^{2}}\left(1+\frac{{\omega }_{ce}{\omega }_{ci}}{{\omega }_{t+}}\right){\alpha }_{+}{A}_{00+}{A}_{00+}^{*}
46

and

{\alpha }_{tt+}=\frac{{\omega }_{pe }^{2}{\omega }_{p}{k}_{0+}{\omega }_{ce}{\mu }^{*}}{2{\omega }_{0+}^{2}{c}^{2}{\gamma }^{2}{k}_{p}}\frac{1}{\left(1-\frac{{\omega }_{ce}}{{\omega }_{t+}}\right)\left(1-\frac{{\omega }_{ce}}{{\omega }_{0+}}\right)\left[\left(1-\frac{{\omega }_{ce}}{{\omega }_{t+}}\right)-\left(1-\frac{{\omega }_{ce}}{{\omega }_{0+}}\right)\right]}{\alpha }_{+}{A}_{00+}{A}_{00+}^{*}
47

The amplitude of THz radiation can be obtained by solving eq. (45) with appropriate boundary conditions.

4 Numerical Results And Discussion

The following set of laser and plasma parameters have been used to perform numerical calculations:

ω_0 = 1.778×10^{15}rad/s, ω_p = 2.398×10^{14}rad/s, r_0 =15μm, ω_{ce} = 0.1ω_0, 0.2ω_0 and 0.3ω_0, ω_{p0} = 0.03ω_0, v_{th} = 0.2c, \alpha {E}_{00}^{2}=1, 1.5 and 2 corresponding to intensities 1.21 × 10^{18}W/cm^2, 2.72 × 10^{18}W/cm^2 and 4.84 × 10^{18}W/cm^2 respectively, b = 0, 0.4, 0.6 and 0.8, and μ = 0.2. For the initial wave front of the beam, the initial conditions for f_{0+} are: {\left.{f}_{0+}\right|}_{z=0}=1 and df_{0+}/dz = 0.

When an intense cosh-Gaussian laser beam propagates through a collisionless magnetized plasma, the refractive index/dielectric constant of plasma is modified due to the relativistic variation of mass and the beam suffers self-focusing. The two terms on the right-hand side of Eq. (22) describe the divergence and convergence of the laser beam, respectively. When the magnitude of the converging term exceeds the diverging term, the beam becomes self-focused in the plasma. Equations (22) and (23) describe the intensity profile and beamwidth (focusing/defocusing) of a cosh-Gaussian laser beam in plasma, when relativistic nonlinearity operates in the extended-paraxial region. It is clear from Eq. (22) that the intensity profile of cosh-Gaussian laser beam in extended-paraxial region depends on the

beamwidth parameter (f) and the coefficients of r^2 and r^4 respectively. In addition, Eqs. (22) and (23) show the direct proportionality between the A_{00} and E_{00}. Numerical computation of the Eqs. (19, 20, 23 and 24) have been carried out to understand the self-focusing behavior of the cosh-Gaussian laser beam in plasma. We have solved Eq. (22) numerically with the numerical computation of Eqs. (19), (20), (23), and (24) to obtain the variation in intensity of the cosh-Gaussian laser beam with the normalized distance of propagation. The results are shown in Figures (1-4).

Figure 1 shows the intensity profile of a cosh-Gaussian laser beam in plasma with the normalized distance of propagation(ξ), when relativistic nonlinearity is functional in the paraxial ($a_2 = a_4 = 0$) and extended-paraxial ($a_2 \neq a_4 \neq 0$) regions. It is clear that the intensity of the cosh-Gaussian laser beam increases in the extended-paraxial region. The is because that the focusing of the cosh-Gaussian laser beam becomes faster in the extended-paraxial region than in the paraxial region due to the involvement of off-axis parts ($a_2 \neq a_4 \neq 0$). The maximum intensity of the cosh-Gaussian laser beam increases by a factor of about 2.3 in the extended-paraxial region. Figure 2 shows the variation in the intensity of the cosh-Gaussian laser beam in plasma with the normalized propagation distance for different values of b, when relativistic nonlinearity is operated in the extended-paraxial region. Because of the strong self-focusing of the cosh-Gaussian laser beam in the plasma at high values of b, the laser beam intensity increases with increasing values of b. It is also clear from Fig. 2 that the intensity of laser beam is minimum at $b = 0$. This is because the beam becomes Gaussian at $b = 0$ like a dark ring. In this case, the beam intensity is maximum on the axis and the propagation length of the beam is reduced. On the other hand, when $b \neq 0$, the beam behaves like a bright ring. The intensity of the beam is maximum on a ring and the propagation length of the beam increases. Thus, the decentered parameter (b) plays a very important role in improving the self-focusing of the cosh-Gaussian laser beam in the plasma.

Figure 3 shows the variation in the intensity of the cosh-Gaussian laser beam in plasma with the normalized propagation distance for different values of the cyclotron frequency (ω_{ce}), when the relativistic nonlinearity is operative in the extended-paraxial region. It is observed that the beam intensity increases significantly with increase in the value of ω_{ce}. This is due to the fact that the extent of self-focusing of the beam increases with increase in ω_{ce}. Figure 4 displays the variation in the intensity of the cosh-Gaussian laser beam in plasma with the normalized distance of propagation for three different values of the intensity parameter (\alpha {E}_{00}^{2}) in the extended-paraxial region, when the relativistic nonlinearity is functional. It is clear that the normalized intensity of the beam is decreases as the value of \alpha {E}_{00}^{2} increases. This is because the self-focusing length of the beam in the plasma decreases with an increase in \alpha {E}_{00}^{2}. Thus, with an increase in the value of \alpha {E}_{00}^{2} the extent of self-focusing of the beam decreases as the convergence term in Eq. (23) decreases.

Equation (45) describes the origin of THz radiation in a magnetized rippled plasma. It is seen from Eq. (45) that the amplitude of THz radiation depends on the nonlinear current density which in turn depends on the gradient of the intensity of the laser beam as well as the beam width ({f}_{0+}) of the laser beam. At the difference frequency of laser beam and electron plasma wave ({\omega }_{t+}={\omega }_{0+}-{\omega }_{p}, the nonlinear oscillatory velocity of electrons couple with the density ripple produces nonlinear current density at THz frequency. To obtain the amplitude of the generated THz wave, Eq. (45) is solved numerically for the same set of parameters and the results are presented in Figs. 5-8. By controlling these parameters, a higher amplitude of the THz wave can be obtained which leads to high THz radiation.

Figure 5 shows the variation of the amplitude of the emitted THz radiation (E_{t+}/E_{00}) with the normalized distance of propagation in the paraxial and extended- paraxial regions, respectively, when relativistic nonlinearity is functional. It is clear from Fig. 5 that the amplitude of THz radiation increases significantly in the extended-paraxial region. This is

because the amplitude of THz radiation depends on the intensity of the laser beam in the plasma and the laser beam intensity further depends on the self-focusing of the laser beam. Figure 6 displays the normalized amplitude of THz radiation with the normalized propagation distance for different values of b in the extended- paraxial region, when relativistic nonlinearity is functional. The amplitude of THz radiation is minimum at $b = 0$ because the laser beam intensity is minimum for the Gaussian profile. It is clearly shown from Fig. 6 that the amplitude of the emitted THz radiation increases with increasing b and is maximum at the focal points of the laser beam, where the laser beam intensity is maximum at b. It is found that the amplitude of the THz radiation by the flat-topped cosh-Gaussian laser beam increases by a factor of more than two times that of the Gaussian laser beam.

The normalized amplitude of THz radiation with normalized propagation distance for different values of ω_{ce} is shown in Fig. 7, when relativistic nonlinearity operates in the extended- paraxial region. It is observed that the amplitude of THz radiation increases significantly with increase in the value of ω_{ce}. Due to the strong self-focusing of the cosh-Gaussian laser beam in the plasma at different values of ω_{ce}, the laser beam intensity increases which further increases the amplitude of THz wave. Figure 8 shows the amplitude of THz radiation with the normalized distance of propagation for different values of incident laser beam intensity (\alpha {E}_{00}^{2}), when relativistic nonlinearity operates in the extended-paraxial region. It is clear from the Fig. 8 that the amplitude of the THz wave decreases when the intensity of the laser beam increases. This is due to the fact that the extent of self-focusing and the laser beam intensity decreases at higher values of \alpha {E}_{00}^{2}, which also reduces the nonlinear current density and the amplitude of the THz radiation. These results describe the effect of self-focusing of the cosh-Gaussian laser beam on the production of THz radiation in a magnetized plasma.

5 Conclusions

In the present investigation, we have studied the self-focusing of a cosh-Gaussian laser beam in a ripple density magnetized plasma and its effect on THz radiation generation, when the relativistic nonlinearity in the extended-paraxial region is functional. The THz wave frequency has been obtained at the difference in the laser beam frequency and the density ripple frequency. Phase matching is an essential requirement for high power THz radiation generation. The necessary condition for phase matching is fulfilled by the density ripple. Analytical equations have been derived for the beam width/intensity of the cosh-Gaussian laser beam in the plasma, the nonlinear dielectric constant of plasma, the nonlinear current density, and the amplitude of the THz wave. The effects of various laser and plasma parameters such as the decentred parameter (b), the electron cyclotron frequency (ω_{ce}), and the incident laser intensity (\alpha {E}_{00}^{2}) have been analysed on the self-focusing of cosh-Gaussian laser beam and the amplitude of the generated THz radiation. The results have been compared to the paraxial-ray approximation and Gaussian profile of the laser beam. The results show that the self-focusing/intensity of the cosh Gaussian laser beam in the magnetized plasma increases in the extended-paraxial region. Furthermore, the intensity of the cosh-Gaussian laser beam increases at higher values of b and ω_{ce} and decreases with increasing \alpha {E}_{00}^{2} due to the self-focusing behaviour of the beam. The intensity is minimum for Gaussian laser beam ($b = 0$). It is observed that the strong THz radiation is generated by the cosh-Gaussian laser beam in the extended-paraxial region. The amplitude of THz radiation which depends on the self-focusing/intensity of the laser beam in the plasma significantly increases at higher values of b and ω_{ce} and decreases with increasing \alpha {E}_{00}^{2}. Hence this scheme can be considered suitable for generating high-power THz radiation.

Declarations

Disclosures. The authors declare no conflicts of interest.

Data Availability. Data underlying the results presented in this paper are not publicly available at this time but may be obtained from the authors upon reasonable request.

References

1. Akhmanov, S. A., Sukhorukov, A. P., Khokhlov, R. V.: Self-focusing and diffraction of light in a nonlinear medium. Sov. Phys. Usp. **10**(5), 609–636(1968)
2. Amouamouha, M., Bakhtiari, F., Ghafary, B.: Self-focused amplitude modulated super Gaussian laser beam in plasma and THz radiation with high efficiency. Results Phys. **17**(6), 103086(2020)
3. Antonsen, T. M., Palastro, J. P., Milchberg, H. M.: Excitation of terahertz radiation by laser pulses in nonuniform plasma channels, Phys. Plasmas **14**(3), 033107(2007)
4. Bonnaud, G., Brandi, H. S., Manus, C., Mainfray, G., Lehner, T.: Relativistic and ponderomotive self-focusing of a laser beam in a radially inhomogeneous plasma II: Beyond the paraxial approximation. Phys. Plasmas **1**(4), 968–989(1994)
5. Chen, Z. Y.: High field terahertz pulse generation from plasma wakefield driven by tailored laser pulses. Appl. Phys. Lett. **102**(24), 241104(2013)
6. Chen, Z.,Zhou, X.,Werley, C. A., Nelson, K. A.: Generation of high power tunable multicycle teraherz pulses. Appl. Phys. Lett. **99**(7), 071102(2011)
7. Ferguson, B., Zhang, X. C.: Materials for terahertz science and technology. Nature Mater.**1**(1), 26–33(2002)
8. Gupta, D. K., Jain, A.: Terahertz radiation generation by a super-Gaussian laser pulse in a magnetized plasma. Optik **227**(2), 165824(2021)
9. Hamster, H., Sullivan, A., Gordon, S., Falcone, R. W.: Short-pulse terahertz radiation from high-intensity-laser-produced plasmas. Phys. Rev. E, Stat. Phys. Plasmas Fluids Relat. Interdiscip. Top. **49**(1), 671–677(1994)
10. Hassan, M. B., Aljanabi, A. H., Singh, M., Sharma, R. P.: Terahertz generation by the high intense laser beam. J. Plasma Phys. **78**(5), 553-558(2012)
11. Hassoon, K. I., Sharma, A. K., Khamis, R. A.: Relativistic laser self-focusing in a plasma with transverse magnetic field. *Phys. Scr.* **81**(2), 025505(2010)
12. Hussain, S., Singh, M., Singh, R. K., Sharma, R. P.: THz generation by self-focusing of hollow Gaussian laser beam in magnetised plasma. EPL **107**(6), 65002(2014)
13. Hussain, S., Singh, R. K., Sharma, R. P.: Strong terahertz field generation by relativistic self-focusing of hollow Gaussian laser beam in magnetoplasma. Laser Part. Beams **34**(1), 86-93(2016)
14. Kim, K. Y.: Generation of coherent terahertz radiation in ultrafast laser-gas interactions. Phys. Plasmas **16**(5), 056706(2009)
15. Kim, K. Y., Glownia, J. H., Taylor, A. J., Rodriguez, G.: Terahertz emission from ultrafast ionizing air in symmetry-broken laser fields. Opt. Express **15**(8), 4577–4584(2007)
16. Kim, K. Y., Taylor, A. J., Glownia, J. H., Rodriguez, G.: Coherent control of terahertz supercontinuum generation in ultrafast laser–gas interactions. Nat. Photonics **2**(10), 605–609(2008).
17. Konar, S., Mishra, M., Jana, S.: Nonlinear evolution of cosh-Gaussian laser beams and generation of flat top spatial solitons in cubic quintic nonlinear media. Phys Lett. A **362**(5-6), 505-510(2007)
18. Koulouklidis, A. D., Gollner, C., Shumakova, V., Fedorov, V. Yu., Pugžlys, A., Baltuška, A., Tzortzakis, S.: Observation of extremely efficient terahertz generation from mid-infrared two-color laser filaments. Nat. Commun. **11**(1), 292(2020)

19. Kumar, S., Singh, R. K., Singh, M., Sharma, R. P.: THz radiation by amplitude-modulated self-focused Gaussian laser beam in ripple density plasma. Laser Part. Beams **33**(2), 257-263(2015)
20. Kumar, S., Singh, R. K., Sharma, R. P.: Terahertz generation by intense femtosecond Gaussian laser pulse in ripple density plasma. IEEE Trans. Plasma Sci. **44**(5), 769-773(2016)
21. Lee, Y. S., Meade, T., Perlin, V., Winful, H., Norris, T. B.: Generation of narrow-band terahertz radiation via optical rectification of femtosecond pulses in periodically poled lithium niobate. Appl. Phys. Lett. **76**(18), 2505–2507(2000)
22. Leemans, W. P., Geddes, C. G. R., Faure, J., Toth, Cs, Tilborg, J. van, Schroeder, C. B., Esarey, E., Fubiani, G., Auerbach, D., Marcelis, B., Carnahan, M. A., Kaindl, R. A., Byrd, J., Martin, M. C.: Observation of Terahertz Emission from a Laser-Plasma Accelerated Electron Bunch Crossing a Plasma-Vacuum Boundary. Phys. Rev. Lett. **91**(7), 074802(2003)
23. Leemans, W. P., Tilborg, J. van, Faure, J., Geddes, C. G. R., Toth, Cs., Schroeder, C. B., Esarey, E., Fubiani, G.: Terahertz radiation from laser accelerated electron bunches. Phys. Plasmas **11**(5), 2899-2906(2004)
24. Liao, G. Q., Li, Y. T.: Review of Intense Terahertz Radiation from Relativistic Laser-Produced Plasmas. IEEE Trans. Plasma Sci. **47**(6), 3002-3008(2019)
25. Liao, G. Q., Li, Y. T., Li, C., Liu, H., Zhang, Y. H., Jiang, W. M., Yuan, X. H., Nilsen, J., Ozaki, T., Wang, W. M., Sheng, Z. M., Neely, D., McKenna, P., Zhang, J.: Intense terahertz radiation from relativistic laser–plasma interactions. *Plasma Phys. Control. Fusion **59**(1),* 014039*(2016)*
26. Lü, B., Ma, H., Zhang,**:** Propagation properties of cosh-Gaussian beams. Opt. Commun. **164**(4-5), 165-170(1999)
27. Malik, H. K., Singh, D., Kumar, R.: Strong Terahertz radiation generation via wakefield in collisional plasma. J. Taibah Univ. Sci. **14**(1), 1279–1287(2020)
28. Miao, C., Palastro, J. P., Antonsen, T. M.: Laser pulse driven terahertz generation via resonant transition radiation in inhomogeneous plasmas. Phys. Plasmas **23**(6), 063103(2016)
29. Miao*,* C., Palastro*,* J. P.,Antonsen, T. M.: High-power tunable laser driven THz generation in corrugated plasma waveguides. Phys. Plasmas **24**(4), 043109(2017)
30. Mittleman, D. M., Jacobsen, R. H., Nuss, M. C.: T-Ray Imaging. IEEE J. Sel. Top. Quantum Electron **2**(3), 679-692(1996)
31. Mun, J., Yea, Kwon-hae, Jeong, Young Uk, Lee, Y. W., Ahn, P. D., Lee, K., Cha, Y. Ho, Cha, H. Jin, Park, S. Hee, Lee, B. C.: Observation of intense terahertz radiation from a laser-produced relativistic plasma generated on metal and plastic solid targets. J. Korean Phys. Soc. **51**(1), 421-425(2007)
32. Nanda, V., Kant, N.: Strong self-focusing of a cosh-Gaussian laser beam in collisionless magneto-plasma under plasma density ramp. Phys. Plasmas **21**(7), 072111 (2014)
33. Pearson, A. J., Palastro, J. P., Antonsen, T. M.: Simulation of terahertz generation in corrugated plasma waveguides. Phys. Rev. E **83**(5), 056403(2011)
34. Pickwell, E., Wallace, V. P.: Biomedical applications of terahertz technology. J. Phys. D Appl. Phys. **39**(17), R301–R310(2006)
35. Purohit, G., Gaur, B., Raizada, A., Kothiyal, P.: Electron acceleration by a cosh-Gaussian laser beam driven electron plasma wave: extended paraxial theory. Opt. Quant. Electron. **53**(9), 592(2021).
36. Rawat, P., Purohit, G.: Self-focusing of a cosh-Gaussian laser beam in magnetized plasma under relativistic-ponderomotive regime. Contrib. Plasma Phys. **59**(2), 226-235(2019)

37. Rawat, P.,Rawat, V.,Gaur, B.,Purohit, G.: Generation of terahertz radiation by intense hollow Gaussian laser beam in magnetised plasma under relativistic-ponderomotive regime. Phys. Plasmas **24**(7), 073113(2017)
38. Sharma, R. P., Singh, R. K.: Terahertz generation by two cross focused laser beams in collisional plasmas. Phys. Plasmas **21**(7), 073101(2014)
39. Shen, Y. C., Lo, T., Taday, P. F., Cole, B. E., Tribe, W. R., Kemp, W. C.: Detection and identification of explosives using terahertz pulsed spectroscopic imaging. Appl. Phys. Lett. **86** (24), 241116(2005)
40. Shukla, P. K., Sharma, R. P.: Alfvén-wave generation in a beam-plasma system. Phys. Rev. A **25**(5), 2816-2819(1982)
41. Singh, M., Mahmoud, S.T., Sharma, R.P.: Generation of THz radiation from laser beam filamentation in a magnetized plasma. Contrib. Plasma Phys. **52**(4), 243-250(2012)
42. Sodha, M. S., Ghatak, A. K., Tripathi, V. K.: *Self-focusing of laser beams in dielectrics, plasma and semiconductors*. Tata-McGraw-Hill, Delhi (1974)
43. Sodha, M. S., Faisal, M.: Propagation of high-power electromagnetic beams in overdense plasmas: Higher order paraxial theory. Phys. Plasmas **15**(3), 033102(2008)
44. Tani, M., Herrmann, M., Sakai, K.: Generation and detection of terahertz pulsed radiation with photoconductive antennas and its application to imaging. *Meas. Sci. Technol.* **13**(11), 1739-1745(2002)
45. Tilborg, J. van, Schroeder, C. B., Filip, C. V., Toth, Cs, Geddes, C. G. R., Fubiani, G., Huber, R., Kaindl, R. A., Esarey, E., Leemans, W. P.: Temporal Characterization of Femtosecond Laser-Plasma-Accelerated Electron Bunches using Terahertz Radiation. Phys. Rev. Lett. **96**(1), 014801(2006)
46. Tonouchi, M.: Cutting-edge terahertz technology. Nature Photonics **1**(2), 97–105(2007).
47. Tripathi, D., Bhasin, L., Uma, R., Tripathi, V. K.: Terahertz generation by an amplitude-modulated Gaussian laser beam in a rippled density plasma column. Phys. Scr. **82**(3), 035504(2010)
48. Vodopyanov, K. L.: Optical THz-wave generation with periodically-inverted GaAs. Laser Photonics Rev. **2**(1-2), 11–25(2008)

Figures

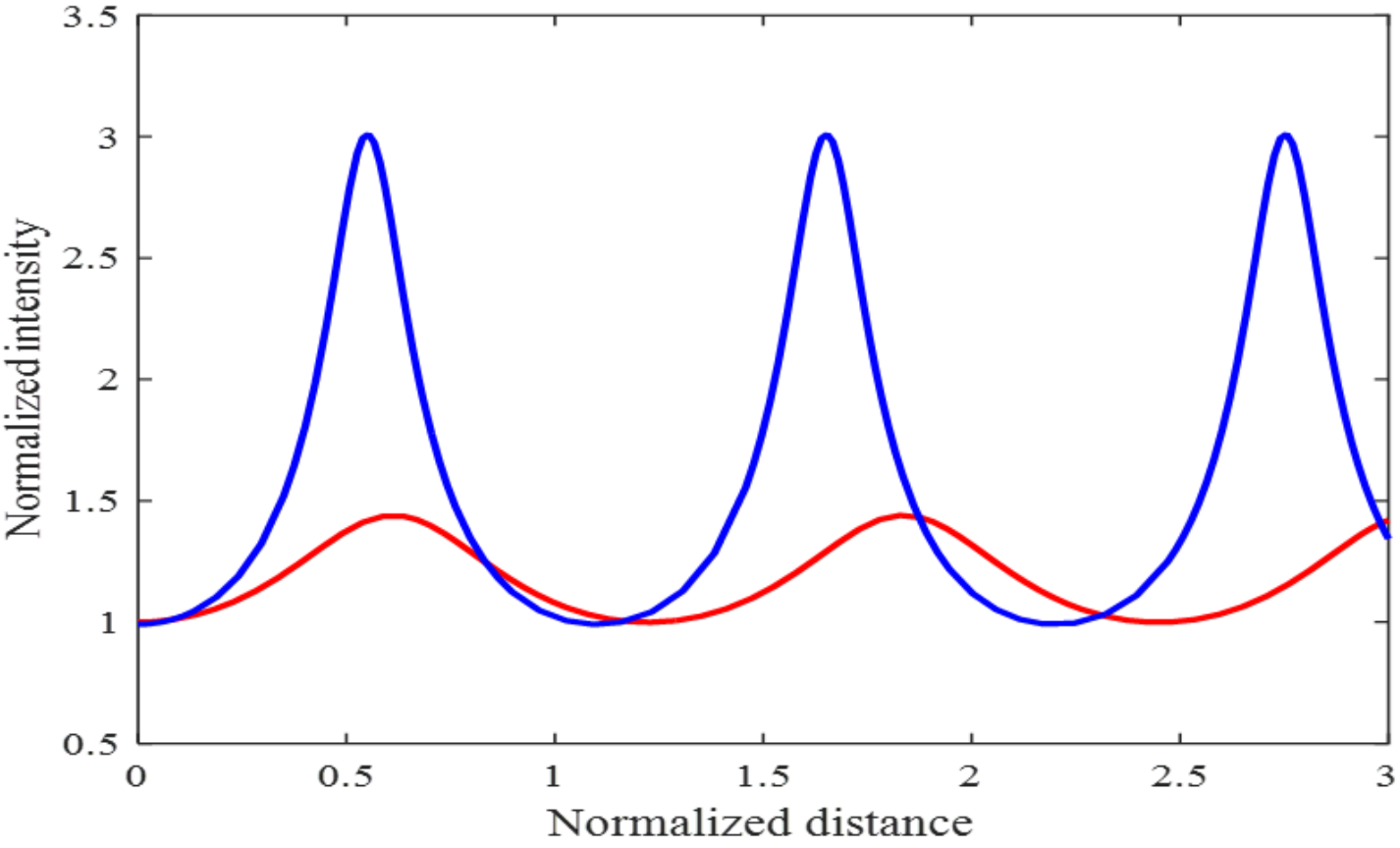

Figure 1

Please see the Manuscript file for the complete figure caption.

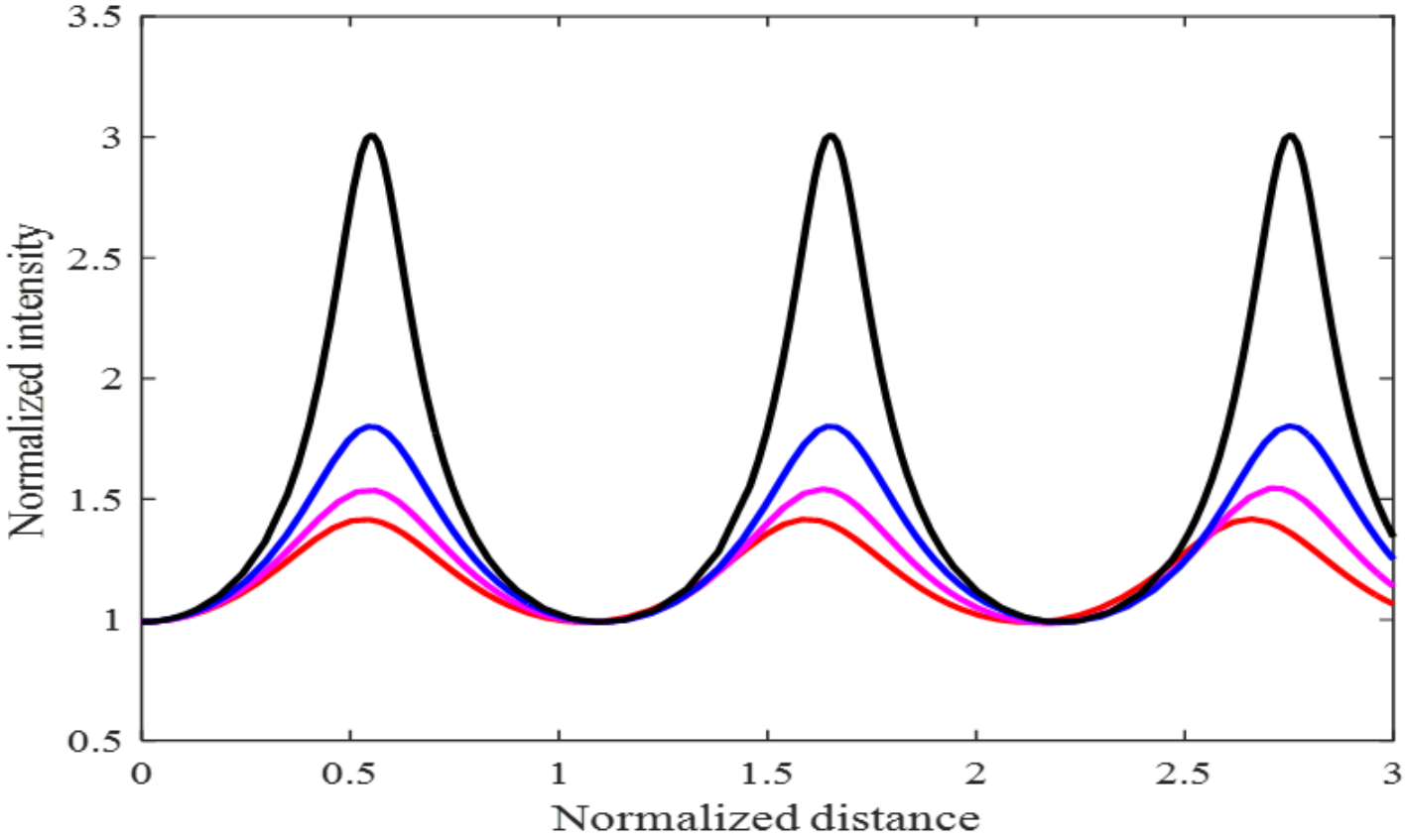

Figure 2

Please see the Manuscript file for the complete figure caption.

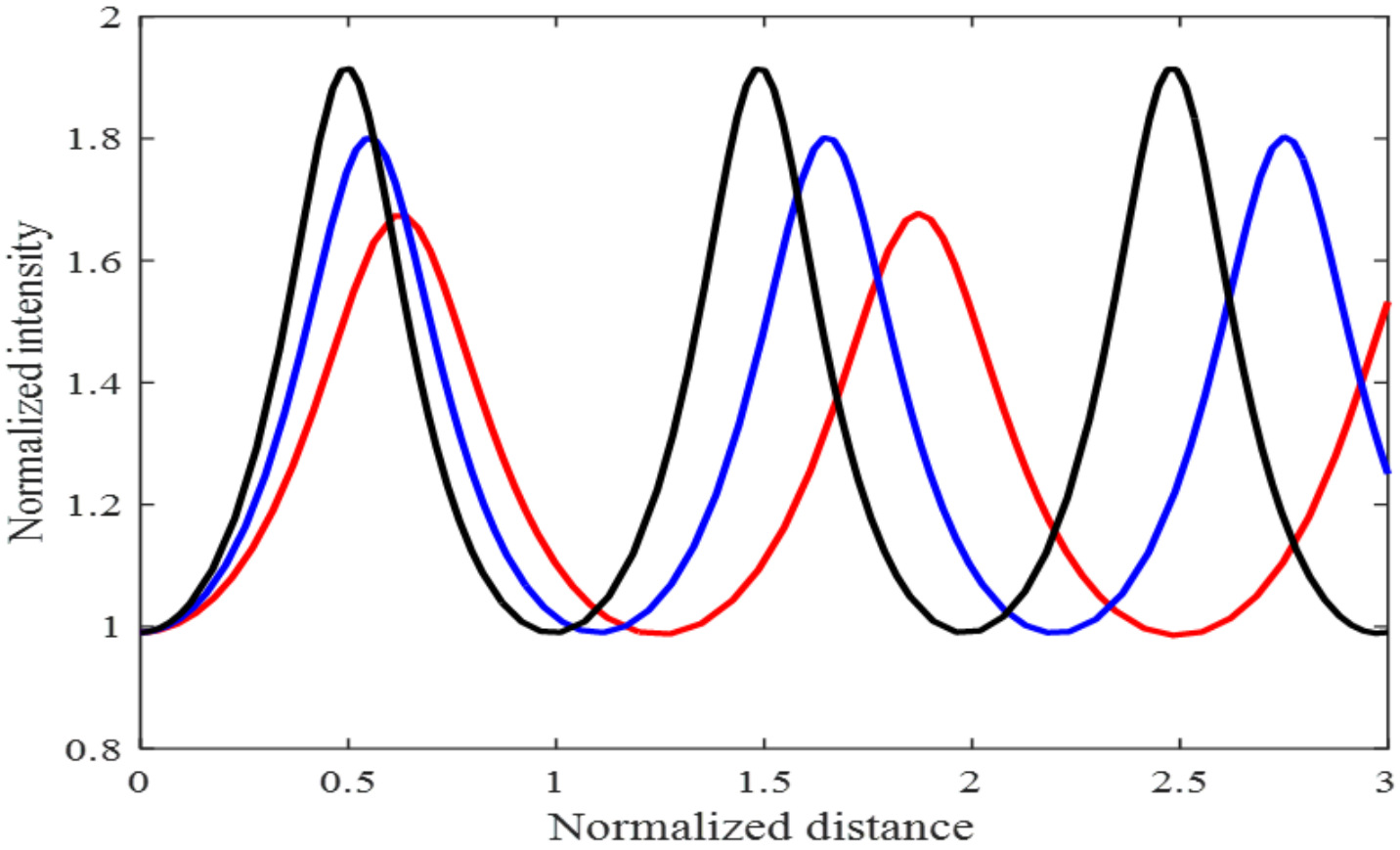

Figure 3

Please see the Manuscript file for the complete figure caption.

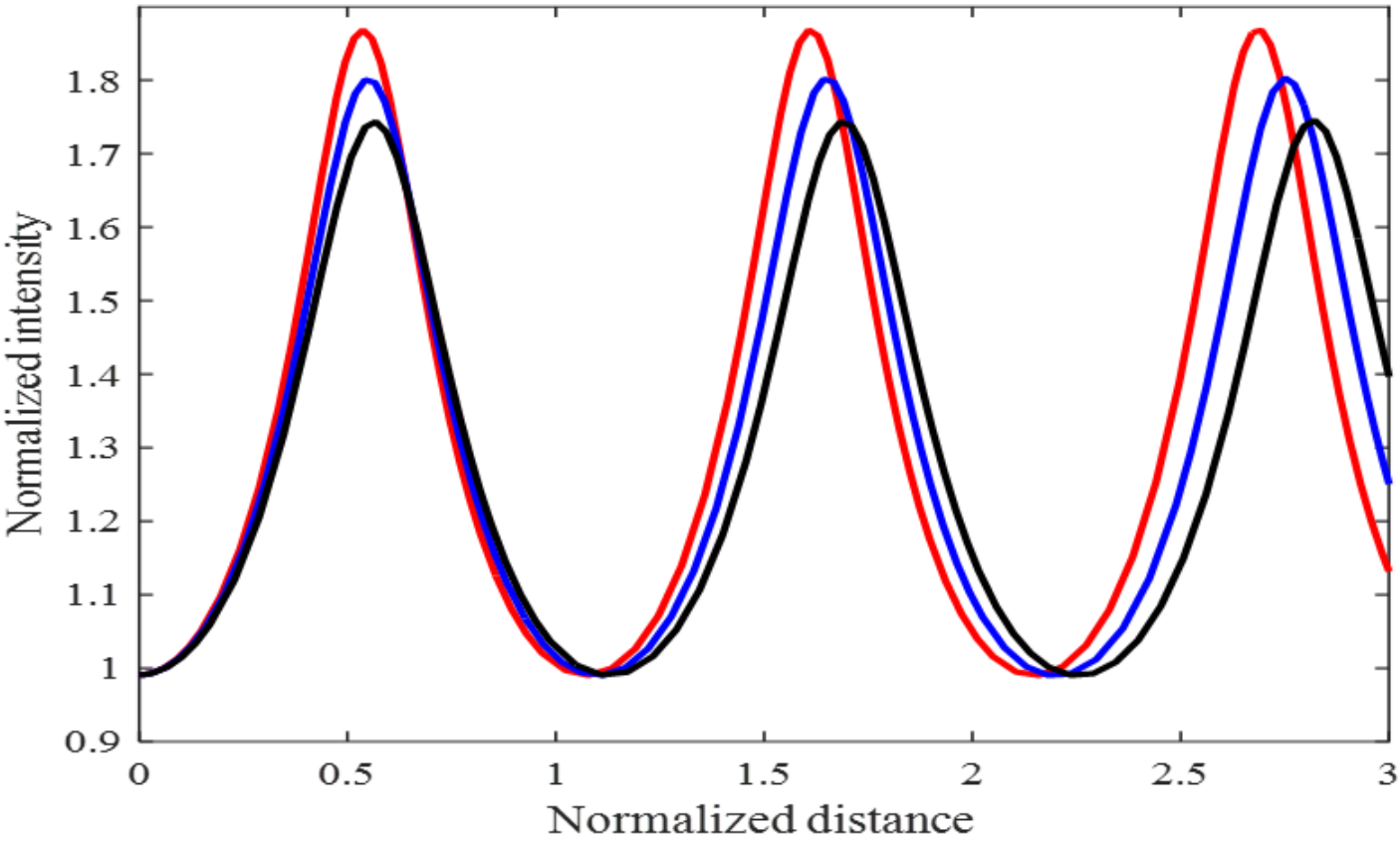

Figure 4

Please see the Manuscript file for the complete figure caption.

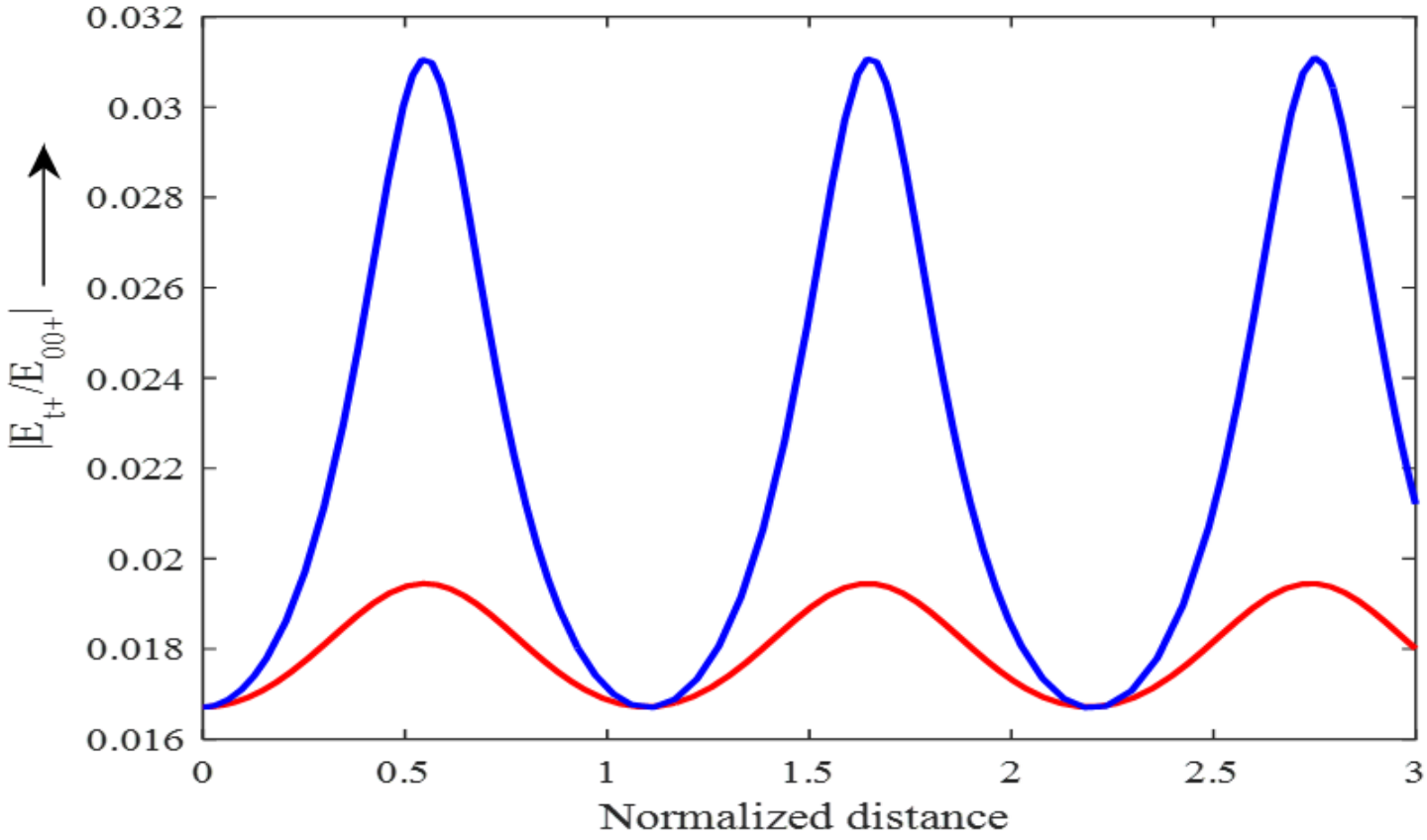

Figure 5

Please see the Manuscript file for the complete figure caption.

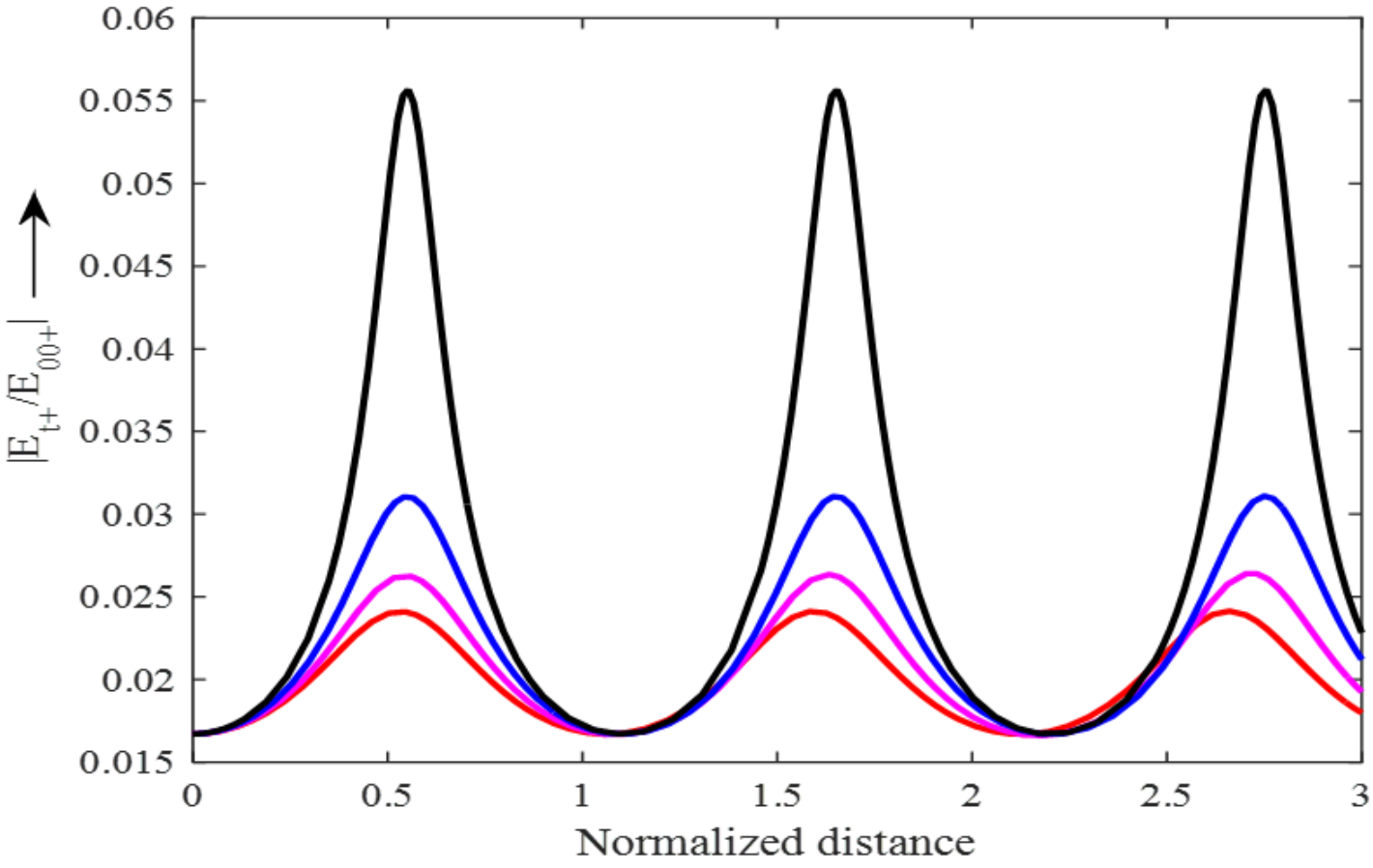

Figure 6

Please see the Manuscript file for the complete figure caption.

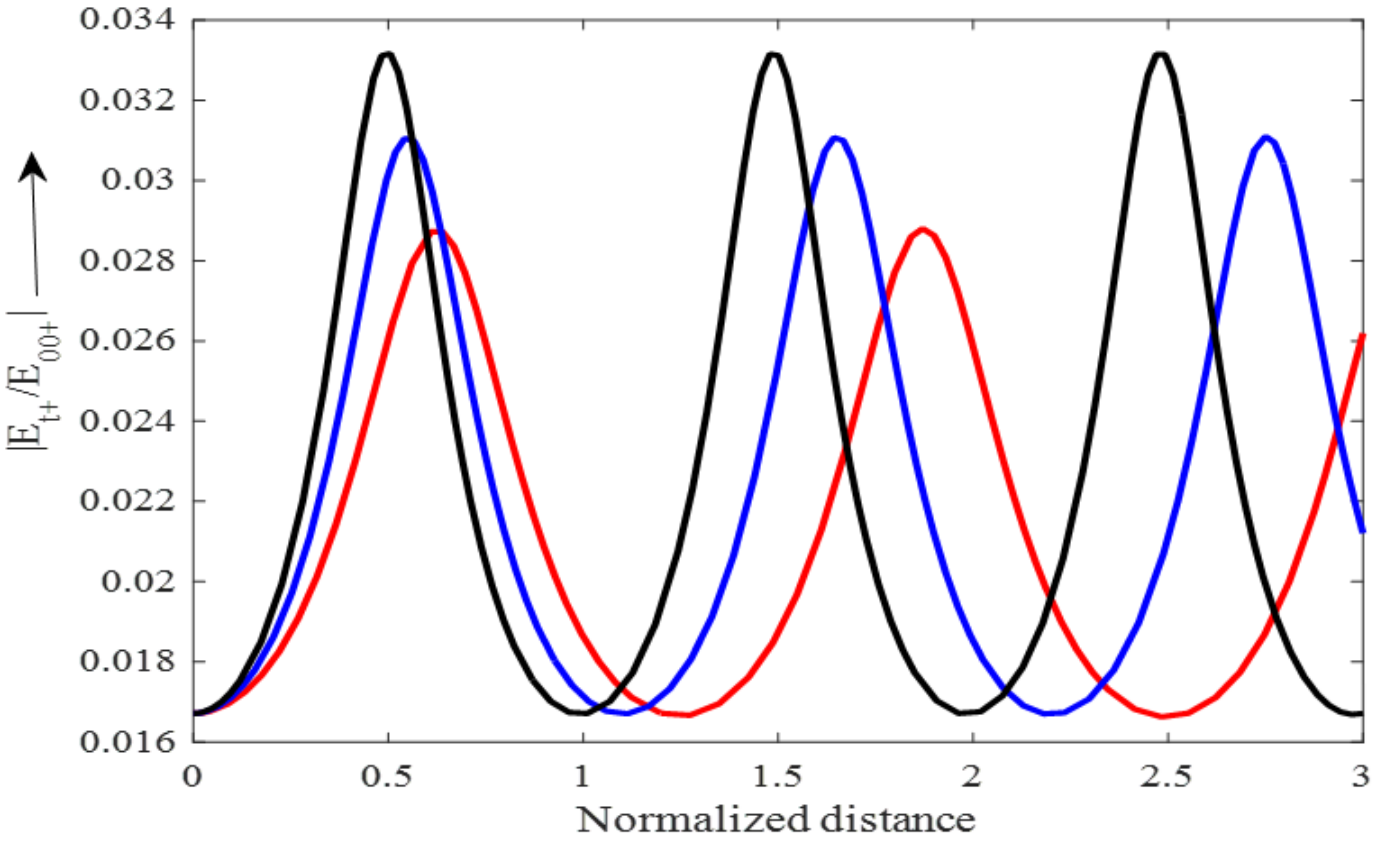

Figure 7

Please see the Manuscript file for the complete figure caption.

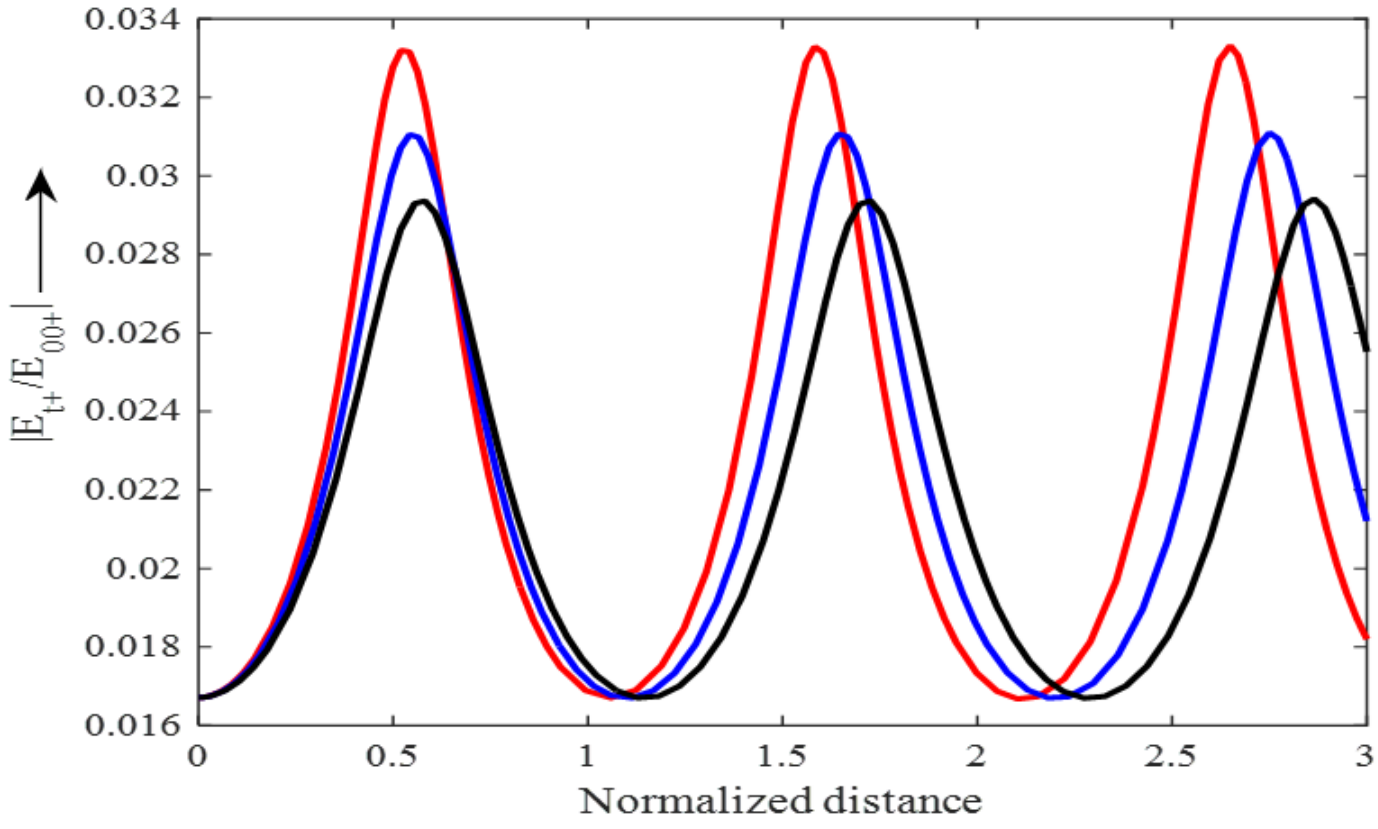

Figure 8

Please see the Manuscript file for the complete figure caption.